2019 Student Design Competition Winners IMS

Wearable/Frugal Microwave Energy Harvesting

©ISTOCKPHOTO.COM/IARTI

Harvesting Electromagnetic Energy in Air

The successful deployment of many emerging technologies, including the Internet of Things (IoT), will require battery-free electric power. Ideally, these emerging technologies will connect multiple, wide-ranging deployed nodes that can independently monitor and collect data, manage resources, and provide services efficiently and in real time. The increased demand for IoT applications in daily life will, in turn, propel demand for billions of sensor nodes [1] for tracking,

Guoyue Xu, Chih-Yu Yang, Janne-Wha Wu, and Chia-Chan Chang

Guoyue Xu (an57520@outlook.com), Janne-Wha Wu (jwwu@ccu.edu.tw), and Chia-Chan Chang (ccchang@ee.ccu.edu.tw) are with the Department of Communications Engineering, National Chung Cheng University, Chia-Yi, Taiwan. Chih-Yu Yang (a29565264@gmail.com) is with the Department of Electrical Engineering, National Chung Cheng University, Chia-Yi, Taiwan.

Digital Object Identifier 10.1109/MMM.2020.2979357

Date of current version: 5 May 2020

assessing awareness and cognitive function, and human–machine interfacing, among other purposes [2]. Sensor nodes have already contributed to the past decade's massive development of low-power electronic devices for daily/weekly continuous operation. However, those devices still rely on batteries for power.

The limitations of batteries include the need for periodic replacement, which can be difficult and expensive [for example, in implantable biomedical devices and wireless sensor networks (WSNs) located in remote and hard-to-reach areas]. Thus, the ability to recharge batteries by collecting renewable environmental energy, such as light, heat, vibration, airflow, and electromagnetic (EM) waves, or even to achieve battery-free power from these sources is a vital goal. For sensor networks that provide continuous monitoring (of physiological states for health care, for example), operation and maintenance would be greatly improved by battery-free modes.

All these requirements are the major driving forces behind the battery-free electronics industry. The energy resources that can be exploited for circuit operation include body motion (such as upper-limb motion [3]); the vibration-based piezoelectric effect [4], [5]; the thermal gradient [6]; and wireless energy in the air [7]. The last option, also called *ambient RF energy harvesting*, is a technique that converts energy from EM waves into electricity: it has attracted significant interest as the field of wireless communication has exploded. Wi-Fi access points and mobile base stations are turning up seemingly everywhere in our living environment, serving as great emitting sources for RF energy harvesting. As summarized [8] in Table 1, worldwide and accessible Wi-Fi applications can provide a 0.18 nW/cm^2 power density for RF energy harvesting.

To emphasize the significance of this perspective, one of the IEEE Microwave Theory and Techniques Society (MTT-S) Student Design Competitions (SDCs), held during the 2019 International Microwave Symposium (IMS) in Boston, encouraged each team to build and demonstrate a wireless energy harvester (WEH) at 2.45 GHz using inexpensive materials. This competition has been held for several years. In 2016, it required the WEH to harvest EM waves from the commercial telephony frequency bands, 700–900 MHz [9]. In 2018, the specification changed to collecting EM waves at 2.45 GHz, and the WEH was required to fit into a hollow cylinder, which required that the WEH bend. A bendable WEH might mean that people could take it with them at all times. The winners' work employed a flexible substrate, Pyralux AP 8555R [10]. Other researchers used more common materials as substrates, such as polyester felt and woven polyester, often used in clothing; based on this, we came up with a new way of thinking about WEHs [11]. As shown in Table 2, for the data of 2016, the efficiency is up to 60% as described in the text (excellent performance in terms of conversion efficiency is reached, with a conversion efficiency of about 50% at 2 W/cm^2 in the whole band and a highest efficiency of up to 60% at the central 800-MHz frequency). For the data of 2018, 5–23% is adopted as described in the text [the efficiency of the final rectenna in the most practical case (bent loaded) ranged 5–23% over the incident power densities required by the competition, 1–10 W/cm^2].

Emerging technologies will connect multiple, wide-ranging deployed nodes that can independently monitor and collect data.

TABLE 1. A summary of the London RF survey measurements [8].

Application	Frequency (MHz)	Average Banded Power Density S_{BA} (nW/cm^2)
Digital television	470–610	0.89
GSM900 (mobile transmitter)	880–915	0.45
GSM900 (base station transmitter)	925–960	36
GSM1800 (mobile transmitter)	1,710–1,785	0.5
GSM1800 (base station transmitter)	1,805–1,880	84
3G (mobile transmitter)	1,920–1,980	0.46
3G (base station transmitter)	2,110–2,170	12
Wi-Fi	2,400–2,500	0.18

TABLE 2. A summary of results from the MTT-S SDCs for energy harvesting.

Year	Frequency	Flexibility	Affects Body Tissue	Power Density (μW/cm^2)	Efficiency	Frugal Material
2016 [9]	700–900 MHz	X	X	1–10	50–60%	X
2018 [10]	2.45 GHz	√	√	1–10	5–23% (bend loaded)	X
2019 (this work)	2.45 GHz	X	√	1–10	5.9–27.7%	√

The limitations of batteries include the need for periodic replacement, which can be difficult and expensive.

In 2019, the competition took the overall weight (<80 g) and size (<8 mm thickness) into consideration. The designed WEH was expected to harvest a power density ranging from 1 to 10 μW/cm^2. In addition, the efficiency figure of merit (EFoM) was considered:

$$\text{EFoM} = 10 * \log_{10}\left[\frac{\left(\frac{P_L(\mu W)}{1(\mu W)}\right)^2}{\frac{D_1(\text{cm})D_2(\text{cm})}{10(\text{cm}^2)}}\right](\text{dB}),$$

where $P_L = V_L^2/R_L$ is the output power taken by the load and $D_1(\text{cm})$ and $D_2(\text{cm})$ are the two largest dimensions of the WEH device. To highlight the potential application in wearable biomedical devices wherein the WEH is closely attached to the human body, a bag of saline water with a dielectric constant of roughly 81 was adopted to mimic body tissue. The off- and on-body harvesting performances were evaluated based on the distance/transfer efficiency.

In this article, we elaborate on our team's design process and experimental results for this application. The concept of an ambient RF energy harvesting system is illustrated in Figure 1. The RF energy in the air is captured by an antenna, followed by matching circuits along with rectifier circuitry. The rectifier is responsible for converting the RF signal to a dc output for the subsequent load. This load can be any self-powered electronic device or a battery. Such a rectifying antenna is also called a *rectenna*, as shown in Figure 1.

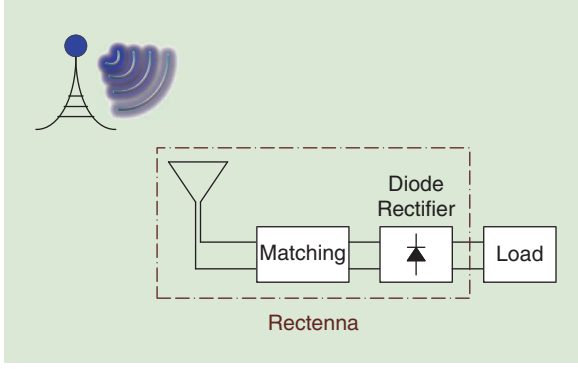

Figure 1. *The operation of an RF energy harvester.*

EM Energy Collecting: Antenna

The receiving antenna is used to collect EM waves in space. With a higher radiation gain and wider operating bandwidth, the antenna can capture more ambient energy. In this design, the patch antenna (also referred to as a *microstrip antenna*) is our primary choice due to its light weight, low profile, simple construction, and compact size. At the same time, the patch antenna suffers from some inherent limitations, including a narrow bandwidth and low gain. Many techniques have been proposed and investigated to overcome those disadvantages, such as using metamaterials and fractal technology to build a small antenna with high efficiency [12]; in addition, the introduction of an air gap (3 mm in this design) in the antenna configuration is useful for improving the bandwidth as well as enhancing the antenna's efficiency [13]. The air gap is inserted between the dielectric substrate and ground plane, creating a multilayer structure. Since the air gap can reduce the equivalent dielectric permittivity, the resonant frequency and radiation properties can be influenced as well. In addition to the bandwidth improvement, the air gap also increases the isolation between the patch radiator and the ground plane, which can moderate the influence of the loading effect from on-body harvesting.

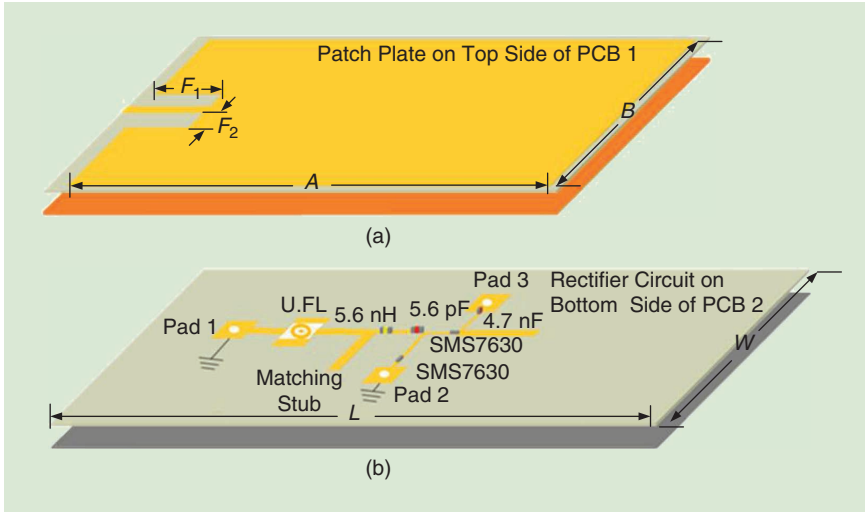

Figure 2. *A 3D description of the energy harvester circuitry. (a) The ground plate on the top side of printed circuit board (PCB) 2. (b) The bottom side of PCB 1. Substrate: 0.8 mm FR4. $F_1 = 8.4$ mm, $F_2 = 2.7$ mm, $A = 53$ mm, $B = 33$ mm, $L = 59$ mm, and $W = 35$ mm. U.FL: the position of an ultrasmall surface-mount coaxial connector for an RF cable.*

Figure 2 shows the proposed rectangular patch antenna's air gap spacing from the ground plane. It is known that the input

impedance at the edge of a patch antenna is relatively high but progressively reduced as the feeding point is moved toward the inside of the patch. Note that it is not necessary to have the standard 50-Ω input impedance because the antenna is connected to the rectifying circuit. However, since the antenna was characterized during the competition using the standard 50-Ω setup, we designed it with 50-Ω impedance. Accordingly, an insert-fed technique was applied in our design. F_1 and F_2 are the length and the width of the insert-fed structure, and A and B are the length and the width of the patch antenna, respectively. The PCB substrate dimension is $W \times L$ mm^2, and the detailed dimensions are also labeled in Figure 2. Two silicon Schottky detector diodes (SMS7630-061) [14] from Skyworks were used.

Figure 3(c) compares the simulated and measured input return loss (S_{11}) with and without the saline water bag. The dashed lines represent the simulation data, while the solid lines represent the measurement data. All the data agree well with each other, while the resonant frequency is shifted slightly down with the addition of the saline water bag. That is because the high dielectric constant of the saline water shortens the guided wavelength so that the antenna size appears more massive than it should be, leading to a lower resonant frequency. In Figure 4 we show the simulated and measured antenna radio pattern using a high-frequency structure simulator and an anechoic chamber for measurements.

Energy harvesting is a technique that converts energy from EM waves into electricity: it has attracted significant interest.

EM Energy Converting: Rectifier Circuit

The rectifier circuit is used to convert the received RF signal into an output dc voltage. Since the overall performance of the WEH relies primarily on the rectifying circuit, the rectifier should have the following characteristics: high efficiency, high sensitivity, low threshold voltage, low leakage current, and small circuit size. We considered a spin diode as an alternative to a Schottky [15] since Schottky diodes tend to underperform when the input power is low. However, spin diodes are still a long way from commercialization. Thus, considering

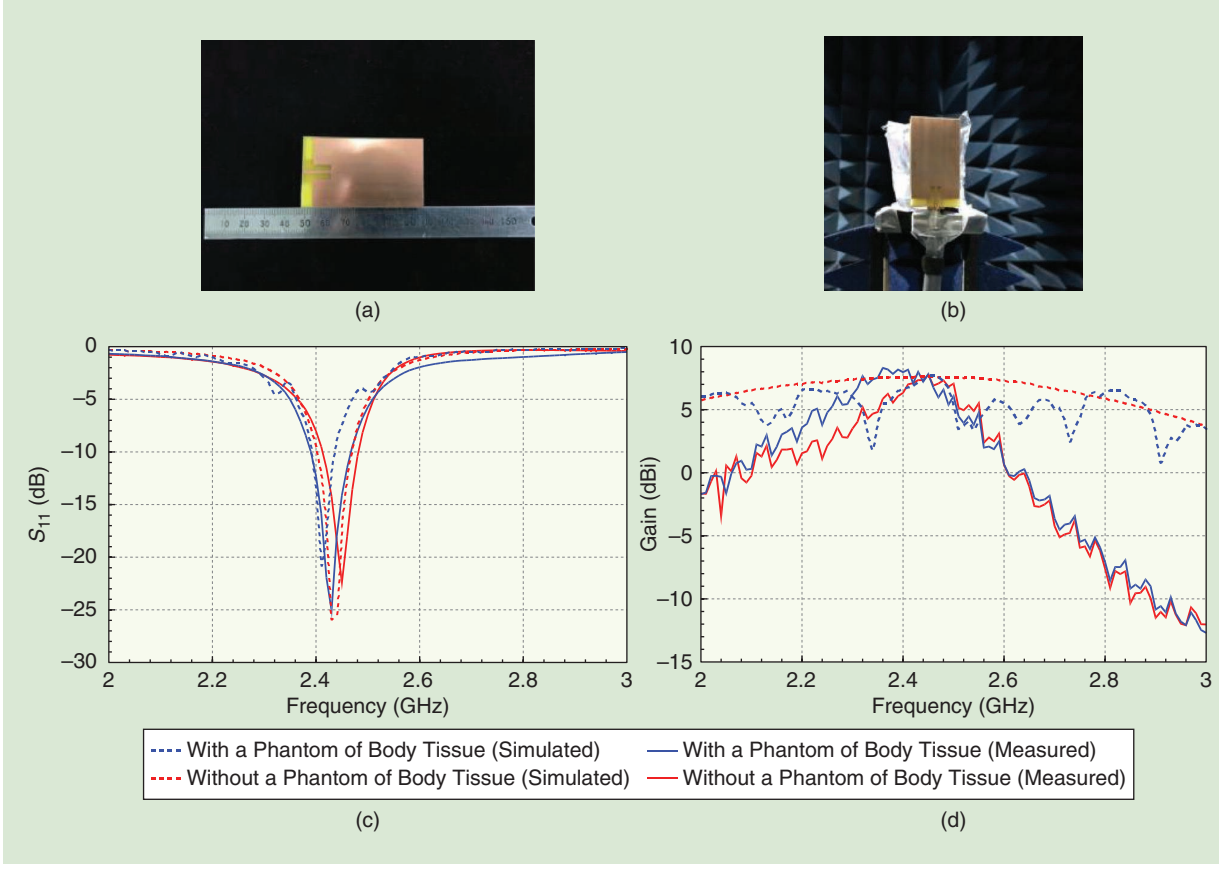

Figure 3. *(a) The antenna. (b) The antenna measured with a phantom of body tissue in the anechoic chamber. The antenna (c) return loss and (d) gain. dBi: decibels relative to an isotropic antenna.*

Wi-Fi access points and mobile base stations are turning up seemingly everywhere in our living environment.

the lack of an off-the-shelf option and the Schottky's switch-like behavior, the Schottky diode (SMS7630-061) [14] was our first choice.

A voltage doubler, which consists of two capacitors and two diodes, is a diode–capacitor pumping circuit. As shown in Figure 5, this kind of rectifier forms a peak rectified by D_1 and C_2, while voltage clamping is achieved by C_1 and D_2. Since the positive and negative cycles of the input RF signals are available to be converted into dc voltage, the total voltage generated is twice what one would have with only a half-cycle input signal. Two zero-bias Schottky detector diodes (SMS7630-061) [14] with a fast switching speed and low forward voltage drop are adopted in this article: they behave with a low barrier height and result in good detector sensitivity without the need for extra bias current in the rectifier. If this rectifier's basic cell is properly cascaded with more stages, the conversion power (efficiency) will increase slightly; however, the required input power level that provides better efficiency will need to increase [16]. Therefore, a one-stage rectifier is adopted in this study to correspond to the actual circumstances. The role of the inductor L and the capacitive stub is to create reactive matching between the antenna and rectifier circuit.

To achieve the lowest possible input power sensitivity of the rectifier, we used Advanced Design System software for the tuning simulation. After the simulation, the real reflection between the antenna, matching network, and rectifier was measured by a vector network analyzer. Fine-tuning was undertaken during this step, and a 5.6-nH series inductor with a parallel capacitive stub was adopted for the final matching network. The antenna and rectifier were connected via a U.FL port.

Figure 6(a) and (b) gives the simulated and measured return loss of the rectifier circuit. The results show a good match between them: 2.48 and 2.36 GHz, respectively. The difference between the measured and simulated results across a higher frequency region may be due to another transmission zero occurring at roughly 2.76 GHz. Figure 6(c) summarizes the available voltage output corresponding to different input powers. The rectifier is fed with different input power levels, from –50 to 5 dB with reference to 1 mW (dBm), and the rectifier output is 800 mV with input power at 0 dBm. Figure 6(d) depicts the loading effect.

Measurement Results of the Integrated Module

The integration of the rectifier and antenna is worth describing since the overall size of the rectenna counted toward the final score in the competition. While a

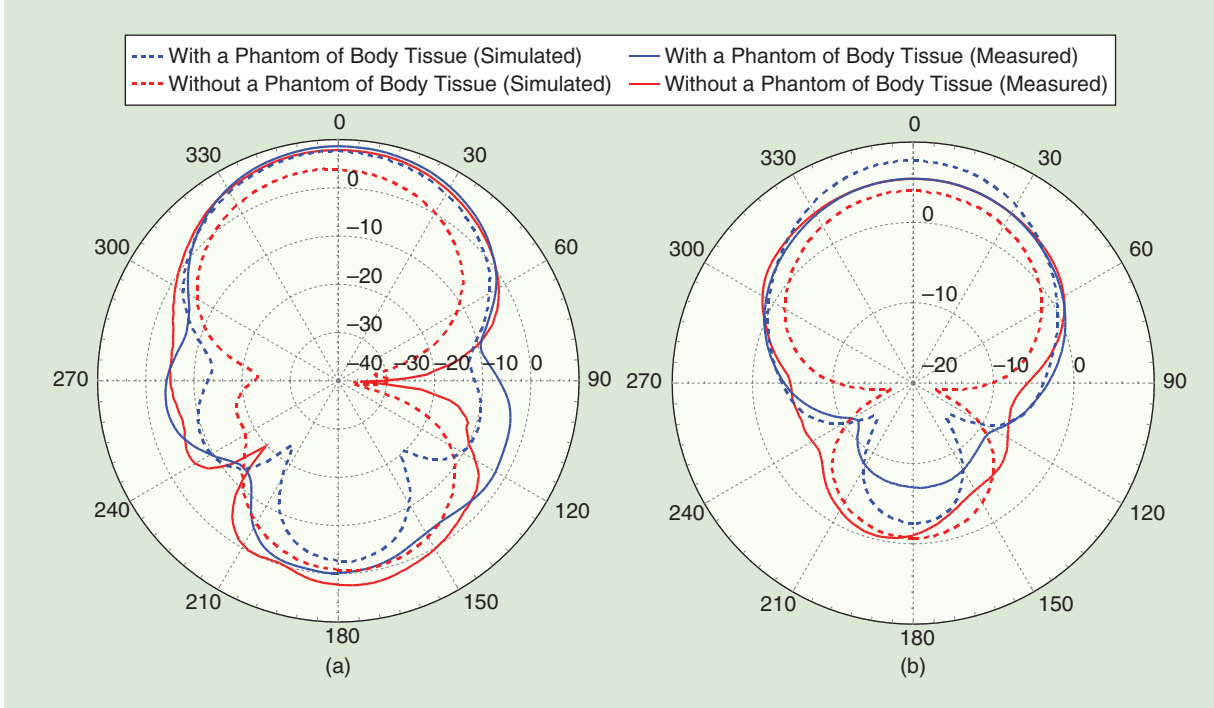

Figure 4. *The simulated and measured radiation pattern in (a) the XZ plane and (b) the YZ plane.*

direct connection is much more straightforward, it will result in a relatively large size. To minimize the size of the module, we had to place the rectifier circuits back to back underneath the antenna, which enabled the ground plane to be sandwiched and shared by both circuits. In this configuration, we slightly increased the height (instead of the length) of the rectenna. Furthermore, since space was of critical concern, we used a cable with miniaturized U.FL connectors instead of the more commonly used subminiature version A connectors to join both circuits. Figure 7(a) and (b) shows the integrated rectenna.

We used a laboratory experiment to validate the performance of the system. A 2.45-GHz signal from a signal generator was transmitted by a horn antenna with a 7-dBi gain, while the designed rectenna was placed in front of it at 0.2 m. We ensured that the antennas were operating in the far field so that the received RF power could be calculated based on the Friis transmission equation:

$$P_r = P_t\left(\frac{\lambda}{4\pi R}\right)^2 G_t G_r,$$

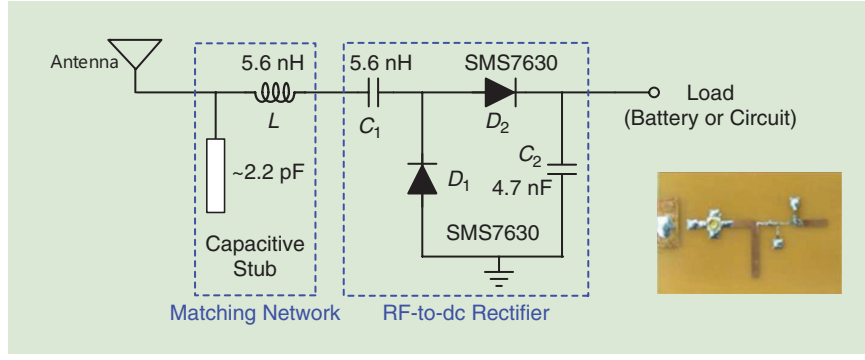

Figure 5. *The RF energy harvester with the antenna, matching network, and RF-to-dc rectifier circuitry used in this article. (The inset shows the built rectifier circuit with a matching network and a miniaturized U.FL connector.)*

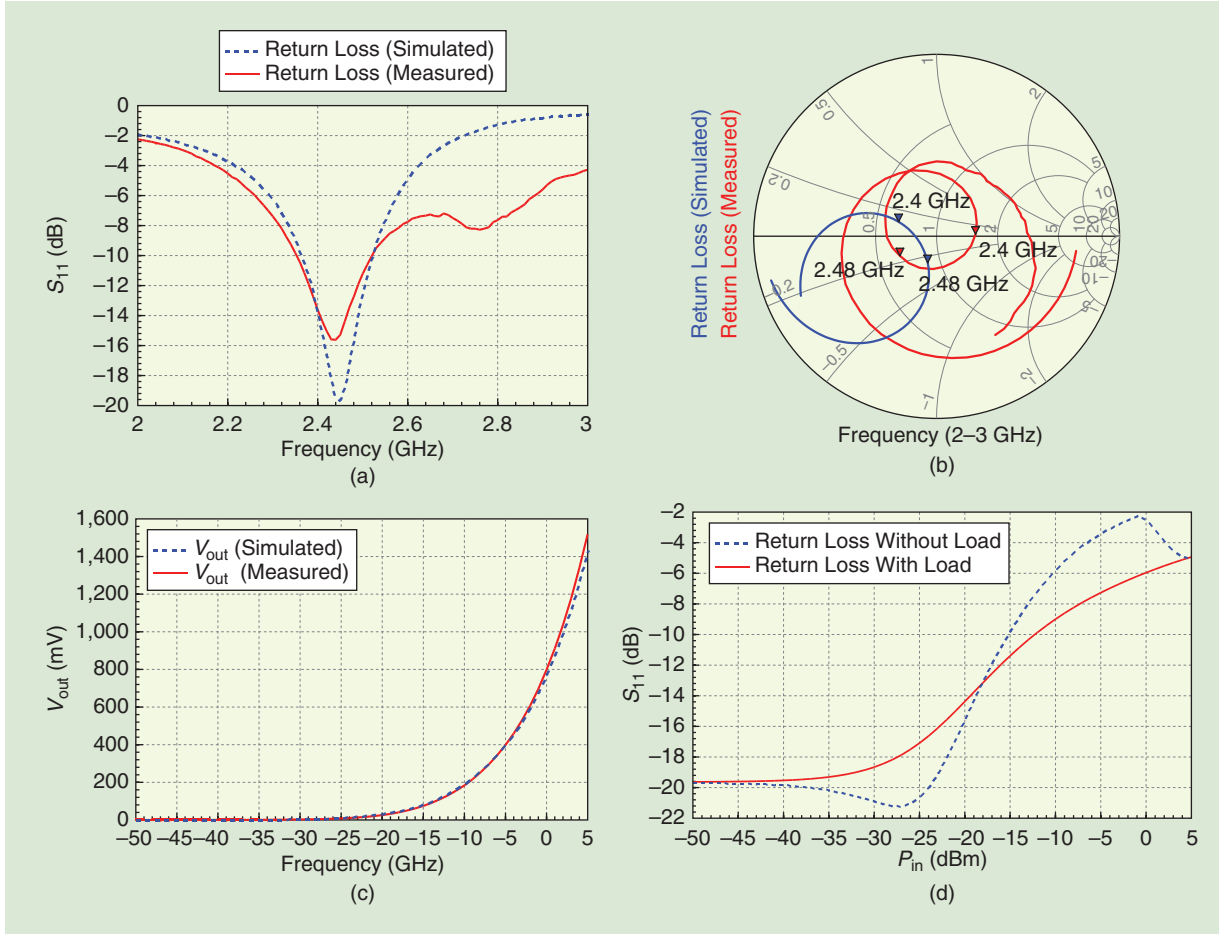

Figure 6. *(a) The return loss of the rectifier. (b) The Smith chart plot of the rectifier's S_{11}. (c) The voltage output of the rectifier, with different power inputs. (d) The loading effect.*

For conversion to a wearable device, the choice of material is an essential consideration.

where P_t is the transmitting power; G_t and G_r are the antenna gain for the transmitting antenna and receiving antenna, respectively; R is the link distance; and λ is the wavelength at the operating frequency.

When the received power is known, the RF-to-dc conversion efficiency can also be calculated. However, the RF-to-dc conversion depends on the load resistor value. In our experiment, a variable resistor was used to measure the preferable load value, which was found to be 2 kΩ:

$$\text{Efficiency}_{\text{RF-DC}} = \frac{P_{\text{dc}}}{P_{\text{RF}}} = \frac{V_{\text{dc}}^2 / R_L}{P_{\text{RF}}}.$$

Considerations for Wearable Energy Harvesting

For conversion to a wearable device, the choice of material is an essential consideration. The antenna's conductivity needs to be high, and, simultaneously, the substrate needs to offer low permittivity and a low loss tangent. However, as a material's flexibility increases, its conductivity tends to decrease, so improving the flexible material's conductivity is the main problem. Polymer-based material mixed with other conductive material seems to be a possible choice since polymer-based materials have good wettability and stretch. For example, a composite of polymer-based fiber and silver [17] presents one possibility for a highly stretchable circuit. Table 3 summarizes the dielectric features of some of the textile materials that have been used as substrates at under 2.4 GHz. As the table suggests, ethylene-vinyl acetate (EVA) in an elastomeric cloth manufactured with silver as the conductive ingredient is a good choice for a wearable antenna, with a radiation efficiency of up to 96.98%, even after being stretched 25% [20].

Conclusions

In this article, we presented the design procedure for a simple WEH. Two FR4 substrates were bound together with a 3-mm gap to achieve the 2019 Student Design Competition (Figure 8) requirements for the antenna and rectifier. The built antenna and rectifier circuit were measured individually, and they matched the

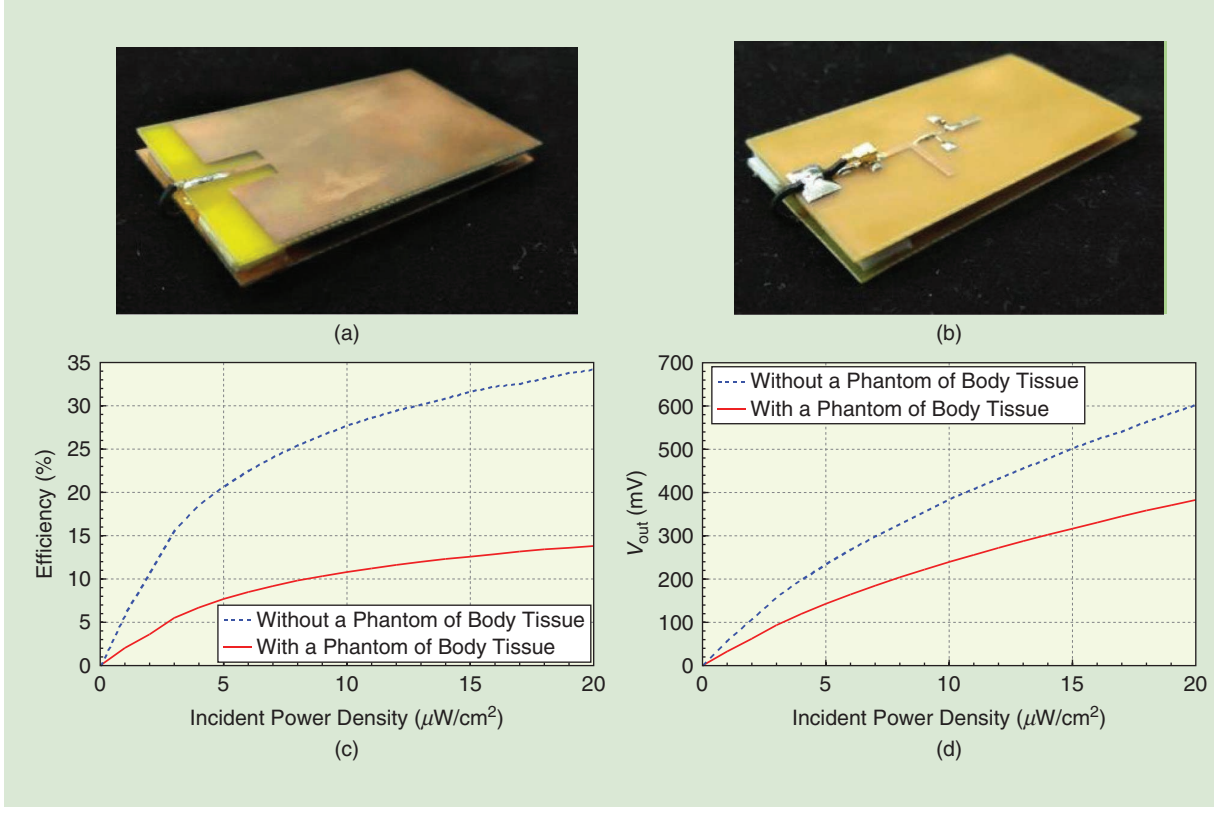

Figure 7. *The final rectenna: (a) front view and (b) back view. (c) The measured efficiency under the normal environment case and the phantom-of-body-tissue case and (d) the dc output under the normal environment case and the phantom-of-body-tissue case.*

TABLE 3. The dielectric features of select textile materials.

Reference	Material	ε_r	tan δ
[18]	Fleece fabric (3 mm)	1.04	—
	Fleece fabric (2.56 mm)	1.25	—
	Felt	1.3	0.02
	Cotton/polyester	1.6	0.02
	Polydimethylsiloxane	3–13	0.02
	Polyamide spacer fabric	1.14	Negligible
	Woolen felt	1.45	0.02
[19]	Aramid substrate (four layers)	1.85	0.015
[20]	Manganese-doped zinc ferrite	7.5	0.025
	Ethylene-vinyl acetate	2.8	0.002

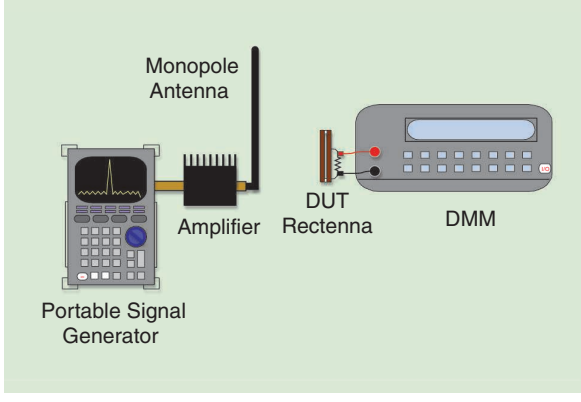

Figure 8. *The testing setup diagram at IMS2019. DUT: device under test; DMM: digital multimeter.*

simulation results well. The measured gain of the antenna is 7.2 dBi at 2.45 GHz. Used in the air without loading, the efficiency of the rectenna can achieve 5.9–27.7% and 1–10 $\mu W/cm^2$. But, under the influence of a phantom of human body tissue, the efficiency is reduced to 2–10.3% and 1–10 $\mu W/cm^2$. In Table 3, candidate flexible materials that might be used for wearable energy harvesting antennas are listed: EVA shows a lower dielectric loss.

References

[1] Y. W. Kuo, C. L. Li, J. H. Jhang, and S. Lin, "Design of a wireless sensor network-based IoT platform for wide area and heterogeneous applications," *IEEE Sensors J.*, vol. 18, no. 12, pp. 5187–5197, June 2018. doi: 10.1109/JSEN.2018.2832664.

[2] M. Gochoo et al., "Novel IoT-based privacy-preserving yoga posture recognition system using low-resolution infrared sensors and deep learning," *IEEE Internet Things J.*, vol. 6, no. 4, pp. 7192–7200, Aug. 2019. doi: 10.1109/JIOT.2019.2915095.

[3] S. Brunner, M. Gerst, and C. Pylatiuk, "Design of a body energy harvesting system for the upper extremity," *Curr. Dir. Biomed. Eng.*, vol. 3, no. 2, pp. 331–334, 2017. doi: 10.1515/cdbme-2017-0067.

[4] G. K. Ottman, H. F. Hofmann, A. C. Bhatt, and G. A. Lesieutre, "Adaptive piezoelectric energy harvesting circuit for wireless remote power supply," *IEEE Trans. Power Electron*, vol. 17, no. 5, pp. 669–676, Sept. 2002. doi: 10.1109/TPEL.2002.802194.

[5] M. H. Ansari and M. Amin Karami, "Piezoelectric energy harvesting from heartbeat vibrations for leadless pacemakers," *in Proc. 15th Int. Conf. Micro and Nanotechnology for Power Generation and Energy Conversion Applications*, Boston. Journal of Physics Conference Series, vol. 660, Bristol, U.K.: IOP Science, Dec. 2015, pp. 1–5. doi: 10.1088/1742-6596/660/1/012121.

[6] C. Vankecke et al., "Multisource and battery-free energy harvesting architecture for aeronautics applications," *IEEE Trans. Power Electron*, vol. 30, no. 6, pp. 3215–3227, June 2015. doi: 10.1109/TPEL.2014.2331365.

[7] S. Gomes et al., "Ultra-small energy harvesting microsystem for biomedical applications," in *Proc. 2014 44th European Microwave Conf.*, Rome, pp. 660–663. doi: 10.1109/EuMC.2014.6986520.

[8] M. Piñuela, P. D. Mitcheson, and S. Lucyszyn, "Ambient RF energy harvesting in urban and semi-urban environments," *IEEE Trans. Microw. Theory Techn.*, vol. 61, no. 7, pp. 2715–2726, July 2013. doi: 10.1109/TMTT.2013.2262687.

[9] V. Palazzi, M. Del Prete, and M. Fantuzzi, "Scavenging for energy: A rectenna design for wireless energy harvesting in UHF mobile telephony bands," *IEEE Microw. Mag.*, vol. 18, no. 1, pp. 91–99, Jan. 2017. doi: 10.1109/MMM.2016.2616189.

[10] A. Abdelraheem, M. Sinanis, S. Hameedi, M. Abdelfattah, and D. Peroulis, "A flexible virtual battery: A wearable wireless energy harvester," *IEEE Microw. Mag.*, vol. 20, no. 1, pp. 62–69, Jan. 2019. doi: 10.1109/MMM.2018.2875629.

[11] S. Adami et al., "A flexible 2.45-GHz power harvesting wristband with net system output from –24.3 dBm of RF power," *IEEE Trans. Microw. Theory Techn.*, vol. 66, no. 1, pp. 380–395, Jan. 2018. doi: 10.1109/TMTT.2017.2700299.

[12] A. Sabban, "Small new wearable antennas for IOT, medical and sport applications," in *Proc. 2019 13th European Conf. Antennas and Propagation (EuCAP)*, Krakow, Poland, pp. 1–5.

[13] K. Ozenc, M. E. Aydemir, and A. Öncü, "Design of a 1.26 GHz high gain microstrip patch antenna using double layer with airgap for satellite reconnaissance," in *Proc. 2013 6th Int. Conf. Recent Advances in Space Technologies (RAST)*, Istanbul, pp. 499–504. doi: 10.1109/RAST.2013.6581259.

[14] Skyworks Solutions Inc., "Surface mount, 0201 zero bias silicon Schottky detector diode," Skyworks Datasheet, SMS7630-061, July 2019. Accessed on: Mar. 22, 2020. [Online]. Available: https://www.skyworksinc.com/-/media/SkyWorks/Documents/Products/101-200/SMS7630_061_201295I.pdf

[15] S. Hemour et al., "Towards low-power high-efficiency RF and microwave energy harvesting," *IEEE Trans. Microw. Theory Techn.*, vol. 62, no. 4, pp. 965–976, Apr. 2014. doi: 10.1109/TMTT.2014.2305134.

[16] I. Chaour, A. Fakhfakh, and O. Kanoun, "Enhanced passive RF-DC converter circuit efficiency for low RF energy harvesting," *Sensors*, vol. 17, p. E546, Mar. 2017. doi: 10.3390/s17030546.

[17] M. Park et al., "Highly stretchable electric circuits from a composite material of silver nanoparticles and elastomeric fibres," *Nat. Nanotechnol.*, vol. 7, no. 12, pp. 803–809, 2012. doi: 10.1038/nnano.2012.206.

[18] R. Salvado, C. Loss, R. Gonçalves, and P. Pinho, "Textile materials for the design of wearable antennas: A survey," *Sensors*, vol. 12, no. 11, pp. 15841–15857, 2012. doi: 10.3390/s121115841.

[19] C. Hertleer, H. Rogier, L. Vallozzi, and F. Declercq, "A textile antenna based on high-performance fabrics," in *Proc. 2nd European Conf. Antennas and Propagation, EuCAP 2007*, Edinburgh, 2007, pp. 1–5. doi: 10.1049/ic.2007.1085.

[20] K. N. Paracha, S. K. Abdul Rahim, P. J. Soh, and M. Khalily, "Wearable antennas: A review of materials, structures, and innovative features for autonomous communication and sensing," *IEEE Access*, vol. 7, pp. 56,694–56,712, Apr. 2019. doi: 10.1109/ACCESS.2019.2909146.